

Simulation Study on Effects of Channel Noise on Differential Conduction at an Axon Branch

Yo Horikawa

Information and Computer Science Laboratory, Faculty of Education, Kagawa University, 1-1 Saiwai-cho Takamatsu, 760 Japan

ABSTRACT Effects of membrane channel noise (random opening and closing of ion channels) are studied on spike conduction at a branching point on an axon. Computer simulation is done on the basis of a stochastic version of the Hodgkin-Huxley cable model, into which the channel noise is incorporated. It is shown that the channel noise makes conduction of spikes into daughter branches random; spikes randomly succeed or fail in conduction into daughter branches. The conduction is then randomly differential even though the forms and properties of daughter branches are the same. The randomness is considerable when the radius of an axon is small ($\sim 1 \mu\text{m}$).

INTRODUCTION

Differential conduction at a branching point on an axon, i.e., success in conduction of spikes into one daughter branch, but failure into the other branch is of wide interest, since it may work as a spatial and temporal filter for a nerve spike train through an axonal tree on a single nerve cell (Chung et al., 1970; Raymond and Lettvin, 1978; Swadlow et al., 1980). Experiments on an axon of the lobster (Grossman et al., 1979a, 1979b) and on the squid giant axon (Stockbridge and Stockbridge, 1988) have obtained direct recordings of the differential conduction of spikes.

From the point of view of studies based on the Hodgkin-Huxley cable model, a theoretical analysis could never explain the differential conduction (Goldstein and Rall, 1974). Computer simulation, however, has shown some mechanisms causing it. One is due to inhomogeneity in membrane properties of daughter branches, particularly in accumulation of potassium ion in the periaxonal space (Parnas and Segev, 1979). The other is due to difference in length of daughter branches, where reflection of currents at boundaries has a significant effect (Stockbridge, 1988). Simulation on axons with synaptic boutons and with complex geometry of bifurcations has also shown that small changes in axonal geometry can cause the differential conduction (Lüscher and Shiner, 1990a, 1990b).

In this paper effects of membrane noise (fluctuations in currents and voltage of nerve membrane) on the differential conduction at an axon branch are considered. The membrane noise is due principally to the channel noise, i.e., random opening and closing of ion channels (DeFelice, 1981; Holden, 1976). Studies on stochastic versions of the Hodgkin-Huxley model, into which the finiteness of the numbers of channels is incorporated, have shown that the channel noise causes considerable variations in the proba-

bility of spike generation (Skaugen and Walløe, 1979; Skaugen, 1980; Clay and DeFelice, 1983) and in the conduction time of spikes along an axon (Horikawa, 1991). The channel noise is thus expected to have an effect on spike conduction at an axonal branch; a spike is conducted into the branch when the membrane voltage of a daughter branch is positively shifted owing to the noise, while the conduction is blocked when the voltage is negatively shifted. Spike conduction into daughter branches is then randomly differential; it is random whether a spike is conducted into both branches, or only one branch, or no branches.

Computer simulation on the stochastic Hodgkin-Huxley model will show that the random differential conduction occurs when the radius of an axon is small ($\sim 1 \mu\text{m}$), where fluctuations in membrane currents and voltage due to the channel noise are large. The conduction can be differential even though each daughter branch has the same membrane properties and the same geometry. Furthermore, correlation of conduction patterns of daughter branches and effects of changes in channel density are studied.

METHODS

Random opening and closing of ion channels have been incorporated into the Hodgkin-Huxley model (Skaugen and Walløe, 1979; Skaugen, 1980; Clay and DeFelice, 1983; Horikawa, 1991). A model axon is discretized into segments of length Δx . The model equations for the membrane voltage $V(x, t)$ of each segment are as follows.

$$\begin{aligned} a/(2R)/(\Delta x)^2 [V(x + \Delta x, t) - 2V(x, t) + V(x - \Delta x, t)] \\ = C \partial V(x, t) / \partial t + g_L [V(x, t) - V_L] \\ + g_{Na}(x, t) [V(x, t) - V_{Na}] + g_K(x, t) [V(x, t) - V_K] \\ g_{Na}(x, t) = \bar{g}_{Na} n_{Na}(x, t) / N_{Na} \\ [= \gamma_{Na} n_{Na}(x, t)] \\ g_K(x, t) = \bar{g}_K n_K(x, t) / N_K \\ [= \gamma_K(x, t)] \end{aligned} \quad (1)$$

where N_{Na} and N_K denote the numbers of Na^+ and K^+ channels in one segment, while $n_{Na}(x, t)$ and $n_K(x, t)$ denote the numbers of open Na^+ and K^+ channels in each segment (γ_{Na} and γ_K are single channel conductances of Na^+ and K^+ channels).

Received for publication 19 October 1992 and in final form 14 April 1993.
Address reprint requests to Y. Horikawa. Tel.: 81-878-61-4141 (ext. 2408);
Fax: 81-878-36-1652; e-mail: horikawa@ed.kagawa-u.ac.jp.

© 1993 by the Biophysical Society
0006-3495/93/08/680/07 \$2.00

The following assumption and approximation are used for calculating the numbers ($n_{Na}(x, t)$, $n_K(x, t)$) of open Na^+ and K^+ channels (Horikawa, 1991). Each channel and each gate in the Hodgkin-Huxley model (Hodgkin and Huxley, 1952) are assumed to act independently. The values of α s and β s are then used as the transition probabilities of opening and closing of corresponding gates. That is, the probability that a closed n gate (m gate, h gate) will open in an interval Δt is given by $\alpha_n \Delta t$ ($\alpha_m \Delta t$, $\alpha_h \Delta t$); the probability that an open n gate (m gate, h gate) will close in Δt is given by $\beta_n \Delta t$ ($\beta_m \Delta t$, $\beta_h \Delta t$). Moreover, to reduce computational time, the numbers of the channels in closed states are approximated by their mean values, which are expressed in terms of n , m , and h .

The following six jumps between open and closed states in Δt are then considered.

Number of open state	← Transition probability →	Number of closed state	
n_{Na}	$-(3\beta_m \Delta t) \rightarrow$	$3m^2(1 - m)hN_{Na}$	
	$\leftarrow (\alpha_m \Delta t) -$		
	$-(\beta_h \Delta t) \rightarrow$	$m^3(1 - h)N_{Na}$	(2)
	$\leftarrow (\alpha_h \Delta t) -$		
n_K	$-(4\beta_n \Delta t) \rightarrow$	$4n^3(1 - n)N_K$	
	$\leftarrow (\alpha_n \Delta t) -$		

That is, we consider only fluctuations in one-step transitions between the open states and the closed states in which one gate is closed. The numbers of the channels changing the state are given by a binomial distribution. It follows that

$$\begin{aligned}
 n_{Na}(x, t + \Delta t) &= n_{Na}(x, t) + n_1(x, t) + n_2(x, t) - n_3(x, t) - n_4(x, t) \\
 n_1(x, t) &\sim \text{Bin}(3m^2(1 - m)hN_{Na}; \alpha_m \Delta t) \\
 n_2(x, t) &\sim \text{Bin}(m^3(1 - h)N_{Na}; \alpha_h \Delta t) \\
 n_3(x, t) &\sim \text{Bin}(n_{Na}; 3\beta_m \Delta t) \\
 n_4(x, t) &\sim \text{Bin}(n_{Na}; \beta_h \Delta t) \\
 n_K(x, t + \Delta t) &= n_K(x, t) + n_5(x, t) - n_6(x, t) \\
 n_5(x, t) &\sim \text{Bin}(4n^3(1 - n)N_K; \alpha_n \Delta t) \\
 n_6(x, t) &\sim \text{Bin}(n_K; 4\beta_n \Delta t)
 \end{aligned}
 \quad (3)$$

$\text{Bin}(N; p)$: binomial distribution.

This simplified version of the stochastic Hodgkin-Huxley model is here applied to spike conduction along an axon with two daughter branches shown in Fig. 1. The left-hand side of the first equation of Eq. 1 at the segments of a branching point is then slightly modified in accordance with Parnas and Segev (1979).

Computation was done with Sun FORTRAN on Sun SPARKstation IPC. Differential equations (Eq. 1 and those for n , m , h in the Hodgkin-

Huxley model) were numerically integrated by the forward-Euler method with the time step Δt . Binomial random variables $n_j(x, t)$ ($j = 1, 2, \dots, 6$) in Eq. 3 were generated using the inverse function method from uniform random numbers drawn from the Sun FORTRAN random number generator. (When the value of $(1 - p)^N$ for $\text{Bin}(N; p)$ was underflowed, $n_j(x, t)$ was generated using the Box-Muller method with the normal distribution $N[Np; Np(1 - p)]$.)

Values of membrane constants except the radii of an axon were same as those in the original Hodgkin-Huxley model (Hodgkin and Huxley, 1952). The radii a of a parent branch and a' of daughter branches were taken to be small, which ranged from 0.05 to 0.8 μm . It is because the intensity of the channel noise is large when the radius is small. Temperature was varied as a parameter to change the safety factor for spike conduction. The length of the segments was: $\Delta x = 0.2\lambda$ ($\lambda = [a/(2Rg)]^{1/2} \approx 457a^{1/2}$ μm : space constant) and an integration time step was: $\Delta t = 2$ μs . The length of a parent branch was 4λ and that of daughter branches was 2λ . The density M_{Na} of Na^+ channels was 300 μm^{-2} ($\gamma_{Na} = 4$ pS) and that M_K of K^+ channels was 30 μm^{-2} ($\gamma_K = 12$ pS) (Conti et al., 1975). Then the numbers of Na^+ and K^+ channels in one segment were: $N_{Na} \approx 574a^{3/2} M_{Na}$ and $N_K \approx 574a^{3/2} M_K$ (a is in microns). Values of the radius a and the corresponding space constant λ and numbers N_{Na} , N_K of ion channels were: $a = 0.05$ μm , $\lambda = 0.1$ mm, $N_{Na} \approx 1.9 \times 10^3$, $N_K \approx 1.9 \times 10^2$; $a = 0.2$ μm , $\lambda = 0.2$ mm, $N_{Na} \approx 1.5 \times 10^4$, $N_K \approx 1.5 \times 10^3$; $a = 0.8$ μm , $\lambda = 0.4$ mm, $N_{Na} \approx 1.2 \times 10^5$, $N_K \approx 1.2 \times 10^4$. The forms of daughter branches were the same throughout simulation, in which case differential conduction never occurs in the absence of noise.

Stimulus current pulses with the interpulse intervals 10 ms were added to the first segment of a parent branch to generate spikes. In each case 1000 spikes were generated and propagated toward a branching point.

In the simulation, intermediate responses conducted into daughter branches occurred since the safety factor is rather low. That is, spike conduction in the decremental manner was observed on daughter branches. There were, however, two peaks in the distribution of maximum values of the voltage at the end of daughter branches caused by the spikes from a parent branch. One is more than 50 mV, and the other is less than 5 mV. The responses were then divided into two classes (conduction success and failure) at some threshold value. The threshold was here set to be 25 mV, and the conduction into daughter branches was then regarded as succeeded if the voltage at the end segment of daughter branches was over 25 mV, and was regarded as failed if not.

The use of a rather coarse space step ($\Delta x = 0.2\lambda$) is due mainly to the restrictions of computational time. It was, however, preliminarily checked that simulation with finer space and time steps ($\Delta x = 0.1\lambda$, $\Delta t = 1$ μs) gives similar results.

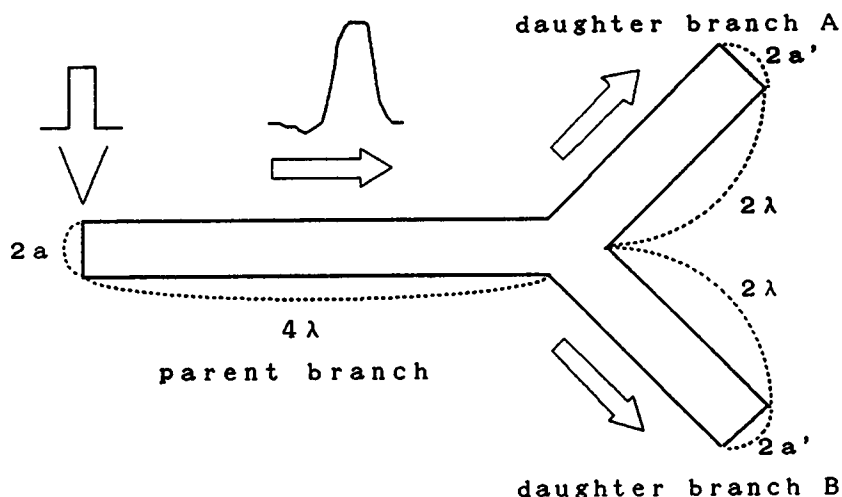


FIGURE 1 Form of a model axon. Length of a parent branch is 4λ and that of daughter branches is 2λ . Radii a' of daughter branches are same.

RESULTS AND DISCUSSION

Random differential conduction on an axon of small radius

First, random differential conduction that occurs on an axon of small radius was shown. The radii of parent and daughter branches were set to be equal, for simplicity. The geometric ratio GR was then fixed to 2. Simulation was done on axons of radii: (I) $a = a' = 0.05 \mu\text{m}$; (II) $a = a' = 0.2 \mu\text{m}$; (III) $a = a' = 0.8 \mu\text{m}$.

Fig. 2 shows a sample of the spatial form of a propagated spike, which is not conducted into the branch A but is conducted into the branch B ($a = a' = 0.05 \mu\text{m}$, temperature: 32.6°C). Note that an apparent cusp at the peak of the spike is seen, since there are only 20 points on the parent branch and they are connected with straight lines.

The channel noise randomly varies the spike form proper to the Hodgkin-Huxley model. While the variations in the spike form are rather small and are hardly seen in the figure, the noise can cause differential conduction at a branching point. Note that spikes are spontaneously generated on an axon of more small radius, in which the intensity of the channel noise is large. The noise intensity on an axon is thus bounded and the variations in the spike form are small compared with those seen in the simulation on spike generation at a small membrane area.

Table 1 shows the numbers of four kinds of conduction patterns, where *11* denotes that a spike is conducted into both daughter branches, *10* and *01* denote that it is conducted into only one branch, and *00* denotes that it is conducted into no branches. The mean probability m that the conduction succeeds is estimated by

$$m = \frac{n_A + n_B}{2n_T} \quad (4)$$

n_T : total number (=1000)

n_A : number of success into the branch A (=11 + 10)

n_B : number of success into the branch B (=11 + 01)

which is also plotted in Fig. 3.

Spikes are conducted into daughter branches in random manners in some temperature regions. The region where the conduction is random ($0 < m < 1$) is narrow when the radius of an axon is larger: from 31.4 to 33.8°C for $a = 0.05 \mu\text{m}$ (I); from 32.3 to 33.1°C for $a = 0.2 \mu\text{m}$ (II); from 32.6 to 32.9°C for $a = 0.8 \mu\text{m}$ (III). The width of the region reaches 2.4°C for $a = 0.05 \mu\text{m}$, while it is only 0.3°C for $a = 0.8 \mu\text{m}$. The randomness of the conduction due to the channel noise is thus considerable for an axon of small radius.

This is attributed to the fact that the effects of the channel noise are of significance as the radius of an axon is smaller. The variances of the channel conductances ($g_{Na}(x, t)$, $g_K(x, t)$) vary inversely as the numbers of the channels (N_{Na} and N_K); thus they are proportional to $a^{-3/2}$.

In the deterministic case ($N_{Na}, N_K \rightarrow \infty$) where the numbers of open channels are calculated with the mean values Np of $n_j(x, t) \sim \text{Bin}(N; p)$ ($j = 1, \dots, 6$) in Eq. 3, which cor-

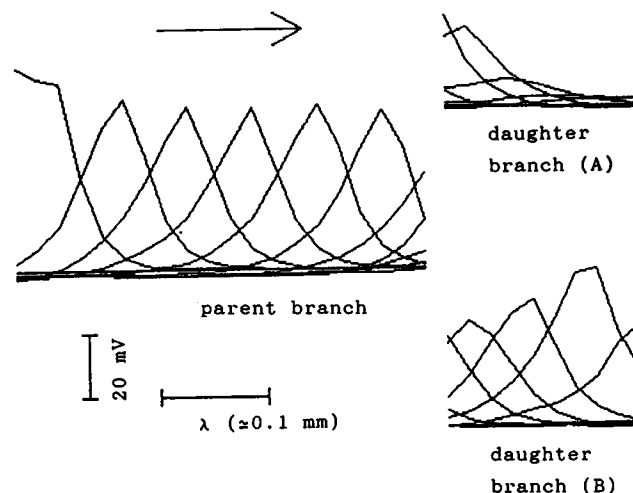


FIGURE 2 Spatial form of a propagated spike in the stochastic Hodgkin-Huxley model. Membrane voltage $V(x, t)$ in the segments are plotted at intervals of 0.2 ms. Radii of all branches are $0.05 \mu\text{m}$ and temperature is 32.6°C . The spike fails in conduction into the branch A but succeeds in conduction into the branch B.

responds to a larger axon, the threshold value of the temperature of conduction success and failure is about 32.75°C (dashed line). The value of the temperature at which the mean probability of conduction success is 0.5 lies between 32.7 and 32.8°C in each case (I–III), which agrees with the deterministic threshold value. The channel noise thus gives a tendency neither to succeed nor fail in the conduction.

The differential conduction into daughter branches corresponds to *10* and *01* patterns in the region of random conduction. Giving the value 1 to success in conduction and the value 0 to failure in conduction, we can estimate the correlation coefficient ρ of the conduction into the daughter branches A and B:

$$\rho = \frac{n_T n_{AB} - n_A n_B}{[n_A(n_T - n_A)n_B(n_T - n_B)]^{1/2}} \quad (5)$$

n_T : total number (=1000)

n_{AB} : number of success into both branches (=11)

n_A : number of success into the branch A (=11 + 10)

n_B : number of success into the branch B (=11 + 01)

which is shown in Table 1. The correlation coefficient is always positive except one value, most values of which range from 0.6 to 0.8. The conduction into the two branches is thus positively correlated and is never independent. The probability that the conduction is differential is smaller than the value $2m(1 - m)$ expected in the independent case.

Correlation of the conduction between daughter branches

Next, to consider the correlation coefficient of the conduction into two branches, the geometric ratio (GR) was

TABLE 1 Conduction into daughter branches

Numbers of patterns*							Numbers of patterns						
Temperature	11	10	01	00	Mean	Corr.	Temperature	11	10	01	00	Mean	Corr.
°C							°C						
	m							m					
	ρ							ρ					
(I) $a = a' = 0.05 \mu\text{m}$							(II) $a = a' = 0.2 \mu\text{m}$ (Continued)						
31.3	1000	0	0	0	1.0000	0.00	33.0	16	5	8	971	0.0225	0.71
31.4	996	0	1	3	0.9965	0.87	33.1	1	5	1	993	0.0040	0.29
31.5	999	1	0	0	0.9995	0.00	33.2	0	0	0	1000	0.0000	0.00
31.6	996	0	2	2	0.9970	0.71							
31.7	975	6	10	9	0.9830	0.53	(III) $a = a' = 0.8 \mu\text{m}$						
31.8	972	8	7	13	0.9795	0.63	32.5	1000	0	0	0	1.0000	0.00
31.9	961	7	9	23	0.9690	0.73	32.6	996	0	1	3	0.9965	0.87
32.0	946	8	19	27	0.9595	0.66	32.7	792	40	53	115	0.8385	0.66
32.1	922	15	18	45	0.9385	0.71	32.8	103	26	34	837	0.1330	0.74
32.2	875	22	21	82	0.8965	0.77	32.9	0	1	0	999	0.0005	0.00
32.3	819	29	28	124	0.8475	0.78	33.0	0	0	0	1000	0.0000	0.00
32.4	729	30	58	183	0.7730	0.75							
32.5	640	49	65	246	0.6970	0.73	(IV) $a = 0.2 \mu\text{m}, a' = 0.05 \mu\text{m}$ (GR = 0.25)						
32.6	552	64	75	309	0.6215	0.70	33.5	1000	0	0	0	1.0000	1.00
32.7	452	61	63	424	0.5140	0.75	33.6	999	0	1	0	0.9995	0.00
32.8	342	67	68	523	0.4095	0.72	33.7	997	1	2	0	0.9985	-0.00
32.9	238	68	49	645	0.2965	0.72	33.8	992	4	4	0	0.9960	-0.00
33.0	168	61	48	723	0.2225	0.69	33.9	988	9	3	0	0.9940	-0.01
33.1	97	44	44	815	0.1410	0.64	34.0	938	28	24	10	0.9640	0.25
33.2	66	24	27	883	0.0915	0.69	34.1	785	65	70	80	0.8525	0.46
33.3	30	19	15	936	0.0470	0.62	34.2	517	100	98	285	0.6160	0.58
33.4	17	11	15	957	0.0300	0.55	34.3	195	69	75	661	0.2670	0.63
33.5	4	5	3	988	0.0080	0.50	34.4	35	28	29	908	0.0635	0.52
33.6	7	6	6	981	0.0130	0.53	34.5	1	5	5	989	0.0060	0.16
33.7	2	0	1	997	0.0025	0.82	34.6	0	1	0	999	0.0005	0.00
33.8	0	1	1	998	0.0010	-0.00	34.7	0	0	0	1000	0.0000	1.00
33.9	0	0	0	1000	0.0000	0.00							
(II) $a = a' = 0.2 \mu\text{m}$							(V) $a = 0.2 \mu\text{m}, a' = 0.8 \mu\text{m}$ (GR = 16)						
32.2	1000	0	0	0	1.0000	0.00	17.1	1000	0	0	0	1.0000	1.00
32.3	997	1	0	2	0.9975	0.82	17.2	994	0	0	6	0.9940	1.00
32.4	986	3	4	7	0.9895	0.66	17.3	992	0	0	8	0.9920	1.00
32.5	926	14	9	51	0.9375	0.80	17.4	787	0	0	213	0.7870	1.00
32.6	800	41	32	127	0.8365	0.73	17.5	520	0	0	480	0.5200	1.00
32.7	532	48	54	366	0.5830	0.79	17.6	56	0	0	944	0.0560	1.00
32.8	285	53	56	606	0.3395	0.76	17.7	14	0	0	986	0.0140	1.00
32.9	83	36	40	841	0.1210	0.64	17.8	3	0	0	997	0.0030	1.00
							17.9	0	0	0	1000	0.0000	1.00

* Success in conduction into both branches (11), only into branch A (10), only into branch B (01), and into no branches (00) (total: 1000).

changed. The following values of the radii of parent (a) and daughter (a') branches were used. (IV) $a = 0.2 \mu\text{m}$, $a' = 0.05 \mu\text{m}$ (GR = 0.25); (V) $a = 0.2 \mu\text{m}$, $a' = 0.8 \mu\text{m}$ (GR = 16). Note that conduction failure at a branching point of geometric ratio less than 1 never occurs when a spike can be propagated along a uniform axon. The propagation of a spike even on a parent branch is the decremental conduction (Cooley and Dodge, 1966; Sabah and Leibovic, 1972) when the geometric ratio is 0.25 (IV), where temperature is so high that the safety factor is low enough to cause conduction failure into daughter branches. Even in this case, the distribution of the maximum voltage at the end of daughter branches had two peaks; one corresponds to the generation of a decrementally conducted spike and the other corresponds to the conduction block at the branching point. The conduction into daughter branches was thus divided into success and failure with the voltage threshold (25 mV), as previously mentioned.

Results are shown in Table 1 (IV and V). The temperature region of random conduction ranges from 33.6 to 34.6°C when the geometric ratio is 0.25 (IV), and ranges from 17.2 to 17.8°C when the geometric ratio is 16 (V). The width of

the random regions is decreased as the radii of daughter branches are larger: 1.0°C for $a' = 0.05 \mu\text{m}$ (IV), 0.8°C for $a' = 0.2 \mu\text{m}$ (II), and 0.6°C for $a' = 0.8 \mu\text{m}$ (V). This is consistent with the relation between the intensity of the channel noise and the radius of an axon, although the width of the regions may not be appropriate for comparison, since the absolute values of the temperature are different.

Values of the correlation coefficient ρ are about 0.5 when the geometric ratio is 0.25 in the region of the moderate values of the mean conduction probability. The correlation coefficient is smaller than that when the geometric ratio is 2 (I–III). All values of the correlation coefficient are 1.0, however, when the geometric ratio is 16. The conduction into daughter branches is then random but never differential (the numbers of 10 and 01 patterns are zero). The correlation coefficient is expected to be increased as the radii of daughter branches are larger and the geometric ratio is larger. The conduction is thus less differential as the geometric ratio is larger.

It is intuitively expected that the noise on a parent branch has a common effect on the conduction into both daughter

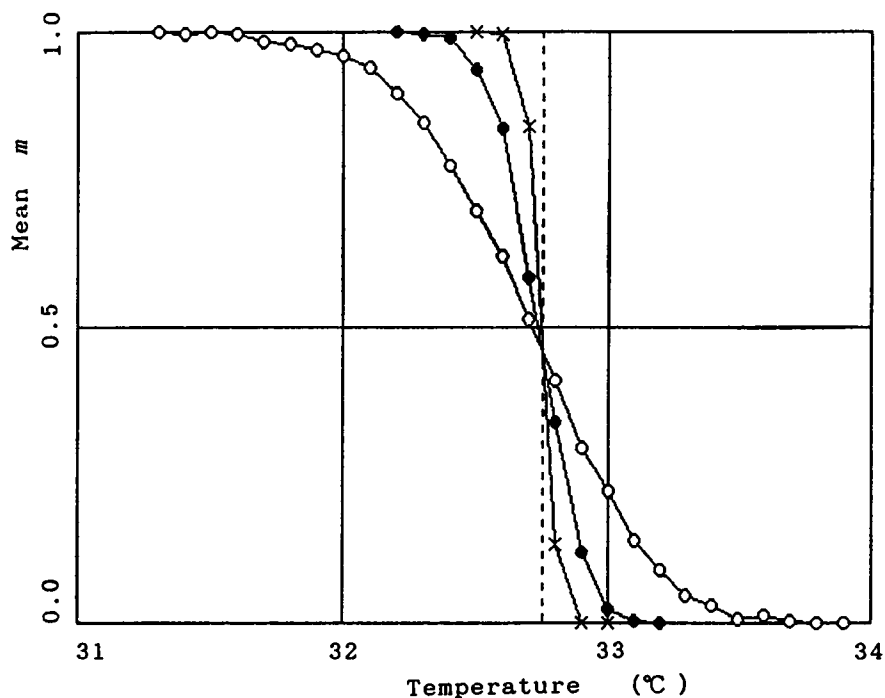


FIGURE 3 Mean probability m that a spike succeeds in conduction into daughter branches. Radii of branches are: $a = 0.05 \mu\text{m}$ (\circ), $a = 0.2 \mu\text{m}$ (\bullet), $a = 0.8 \mu\text{m}$ (\times). A vertical dashed line denotes the threshold of conduction success in the absence of the noise. The region in temperature where the conduction is random widens as the radii are smaller.

branches, while the noise on each daughter branch has an effect mostly on the conduction into each branch. That is, the conduction becomes almost independent ($\rho \rightarrow 0$) as the noise on a parent branch is smaller than that on daughter branches, while the conduction becomes hardly differential ($\rho \rightarrow 1$) as the noise on a parent branch is larger than that on daughter branches. A smaller geometric ratio means that the intensity of the noise on a parent branch is smaller than that of daughter branches and thus tends to make the conduction differential.

The correlation of the conduction between daughter branches can be high also when an axon is bifurcated into more than two branches. It is because the noise on other branches than the two branches considered has a common effect. Simulation on an axon with three daughter branches can show that values of the correlation coefficient between two branches range from 0.8 to 0.9, which are larger than those shown in Table (I–III).

Effects of channel density

Here the relation of the effects of channel density (and single channel conductance) to those of temperature and the radius of an axon is discussed. This discussion shows that differential conduction, due to the channel noise, occurs under more moderate conditions than those in the simulation, when channel density is small.

In the simulation, high temperature above 30°C was needed to lower the safety factor, and small radii less than $1 \mu\text{m}$ were needed to increase the intensity of the channel noise. It is because the channel densities of the squid giant

axon were used ($M_{\text{Na}} = 300 \mu\text{m}^{-2}$, $M_{\text{K}} = 30 \mu\text{m}^{-2}$). It can be shown, however, that lowering channel density makes both the safety factor low and the noise intensity high.

The cable equation for the membrane voltage of an axon is described in a normalized manner (Sabah and Leibovic, 1972):

$$\partial^2 V(y, \tau) / \partial x^2 = \beta^{-1} \partial V(y, \tau) / \partial \tau + I_i(y, \tau)$$

$$\begin{aligned} y &= x/\lambda & (\lambda &= [a/(2R\bar{g})]^{1/2}: \text{space constant}) \\ \tau &= \phi t & (\phi &= 3^{(T-6.3)/10}: \text{factor for temperature}) \end{aligned} \quad (6)$$

where space and time are normalized with the space constant and the temperature factor with a Q_{10} of 3, respectively. Here η_N is a factor multiplying channel densities (e.g., $M_{\text{Na}} \rightarrow \eta_N M_{\text{Na}}$) and η_τ is a factor multiplying single channel conductances (e.g., $\gamma_{\text{Na}} \rightarrow \eta_\tau \gamma_{\text{Na}}$). Note that the maximum channel conductances are then: $\bar{g}_{\text{Na}} \rightarrow \eta_N \eta_\tau \bar{g}_{\text{Na}}$ and $\bar{g}_{\text{K}} \rightarrow \eta_N \eta_\tau \bar{g}_{\text{K}}$.

The safety factor and the noise intensity are related to channel density and single channel conductance in the following way.

First, a factor β in Eq. 6 corresponding to the safety factor is expressed as follows.

$$\beta = \eta_N \eta_\tau / (C\phi) \quad (7)$$

Thus increase in temperature and decrease in both channel density and single channel conductance reduce the safety factor.

Second, the variance σ_I^2 of fluctuations in the current density $I_i(y, \tau)$ due to the channel noise is inversely proportional

to the numbers (N_{Na} , N_K) of channels in one segment of space constant length. Then

$$\sigma_I^2 \propto a^{-3/2} \eta_N^{-1} \quad (8)$$

since N_{Na} , N_K are proportional to $a^{3/2} M_{Na}$, $a^{3/2} M_K$. Decrease in a radius and decrease in channel density thus make the noise intensity high.

Channel density proves to be related to both the safety factor and the noise intensity. That is, decrease in channel density is equivalent to both increase in temperature and decrease in the radius:

$$\begin{aligned} N_{Na} \rightarrow \eta_N N_{Na} &\Leftrightarrow T' \rightarrow T' - 10 \log_3 \eta_N \\ N_K \rightarrow \eta_N N_K &\quad a \rightarrow \eta_N^{-2/3} a \end{aligned} \quad (9)$$

When the channel density is decreased with $\eta_N = 0.1$: $M_{Na} = 300 \mu\text{m}^{-2} \rightarrow 30 \mu\text{m}^{-2}$ (one-tenth that of the squid giant axon), for instance, the temperature threshold and the radius corresponding to those in the simulation (I–III) are changed: $T' \approx 32.7^\circ\text{C} \rightarrow 11.7^\circ\text{C}$ and $a = 0.05\text{--}0.8 \mu\text{m} \rightarrow 0.23\text{--}3.7 \mu\text{m}$, respectively.

Furthermore, it is expected that the channel densities of actual axons are decreased as the radii are smaller (Jack, 1975); rabbit vagus nerve: $M_{Na} \approx 27 \mu\text{m}^{-2}$, $2a \approx 0.3\text{--}1.95 \mu\text{m}$; lobster leg nerve: $M_{Na} \approx 16 \mu\text{m}^{-2}$, $2a \approx 0.2\text{--}30 \mu\text{m}$; garfish olfactory nerve: $M_{Na} \approx 2.5 \mu\text{m}^{-2}$, $2a \approx 0.2 \mu\text{m}$. These values of the channel densities and radii of small axons, principally those of rabbit vagus nerve, fall in the ranges of the above instance. (Temperature regions may be different owing to changes in the safety factor due to single channel conductance.) The channel noise can thus have a significant effect on differential conduction on actual small axons.

Relation to experimental results

Many experiments on the conduction block of spikes at a branching point of an axon have been done (for reviews see Swadlow et al. (1980)). The simulation results in this paper are relevant to past experimental observations.

First, the direct measurement of differential conduction has been done on large axons: the axons of the lobster of diameter $\approx 75 \mu\text{m}$ (Grossman et al., 1979a) and the squid giant axon (Stockbridge and Stockbridge, 1988). The simulation results suggest that the channel noise has little effects on such large axons. Random differential conduction due to the channel noise, however, can be observed when experiment is done on smaller axons of radius $\sim 1 \mu\text{m}$. Furthermore, it is apt to occur on narcotized axons, since decrease in the density of active channels makes the effects of the channel noise large.

Second, frequency-dependent differential conduction of a spike train has been considered in most experiments, while the conduction of a single spike was considered in the simulation in order that other factors than the channel noise were excluded. The frequency-dependent differential conduction gives an axonal tree the function of changing temporal patterns into spatial ones (Chung et al., 1970) and thus is of more interest. Spike frequency (or interspike intervals) is then a

parameter that changes the safety factor for spike conduction, and thus random differential conduction can appear in some regions of the spike frequency. Conduction failure in the refractory period occurs in lower temperature regions than those in the simulation. Furthermore, fluctuations in the period of intermittent conduction observed in the experiment (Raymond and Lettvin, 1978) may be due partly to the channel noise.

Furthermore, actual small axons have properties different from those of the Hodgkin-Huxley model based on the squid giant axon. There are various kinds and different types of ion channels and ion pumps (Hille, 1984; Scriven, 1981). The density and distribution of the ion channels are also varied (Jack, 1975; Waxman and Ritchie, 1985). Accumulative changes in ion concentration, which cause adaptation and accommodation, are of significance principally for the frequency-dependent differential conduction of a spike train. Although these factors need to be considered in order to study the effects of the channel noise more quantitatively, the results obtained in this simulation give rough estimates for them.

CONCLUSION

The computer simulation on the stochastic Hodgkin-Huxley model showed that the channel noise has a considerable effect on spike conduction at a branching point of an axon. The conduction into daughter branches is randomly differential in some temperature regions. The random differential conduction is considerable as the radius of an axon is smaller ($\sim 1 \mu\text{m}$), since the fluctuations in membrane currents due to the channel noise are large. The randomness due to the channel noise is thus inevitable in the differential conduction principally in the terminal region of an axon where small branches are bifurcated.

The simulation showed that the channel noise makes the conduction into daughter branches differential but not preferential, since the forms of daughter branches were the same throughout it. It will be shown in the subsequent paper that the conduction can be preferential when the radii of daughter branches are different.

This work was partly supported by the Sasakawa Scientific Research Grant from The Japan Science Society.

REFERENCES

- Chung, S., S. A. Raymond, and J. Y. Lettvin. 1970. Multiple meaning in single visual units. *Brain Behav. Evol.* 3:72–101.
- Clay, J. R., and L. J. DeFelice. 1983. Relationship between membrane excitability and single channel open-close kinetics. *Biophys. J.* 42:151–157.
- Conti, F., L. J. De Felice, and E. Wanke. 1975. Potassium and sodium ion current noise in the membrane of the squid giant axon. *J. Physiol. (Lond.)* 248:45–82.
- Cooley, J. W., and F. A. Dodge, Jr. 1966. Digital computer solutions for excitation and propagation of the nerve impulse. *Biophys. J.* 6:583–599.
- DeFelice, L. J. 1981. Introduction to Membrane Noise. Plenum Publishing Corp., Inc., New York. 500 pp.

- Goldstein, S., and W. Rall. 1974. Changes of action potential shape and velocity for changing core conductor geometry. *Biophys. J.* 14:731-757.
- Grossman, Y., I. Parnas, and M. E. Spira. 1979a. Differential conduction block in branches of a bifurcating axon. *J. Physiol. (Lond.)*. 295:283-305.
- Grossman, Y., I. Parnas, and M. E. Spira. 1979b. Ionic mechanisms involved in differential conduction of action potentials at high frequency in a branching axon. *J. Physiol. (Lond.)*. 295:307-322.
- Hille, B. 1984. *Ionic Channels of Excitable Membranes*. Sinauer Associates, Sunderland, Massachusetts. 426 pp.
- Hodgkin, A. L., and A. F. Huxley. 1952. A quantitative description of membrane current and its application to conduction and excitation in nerve. *J. Physiol. (Lond.)*. 117:500-544.
- Holden, A. V. 1976. *Models of Stochastic Activity of Neurons*. Springer Publishing Co., Inc., New York. 368 pp.
- Horikawa, Y. 1991. Noise effects on spike propagation in the stochastic Hodgkin-Huxley models. *Biol. Cybern.* 66:19-25.
- Jack, J. J. B. 1975. Physiology of peripheral nerve fibers in relation to their size. *Br. J. Anaesth.* 47:173-182.
- Lüscher, H.-R., and J. S. Shiner. 1990a. Computation of action potential propagation and presynaptic bouton activation in terminal arborizations of different geometries. *Biophys. J.* 58:1377-1388.
- Lüscher, H.-R., and J. S. Shiner. 1990b. Simulation of action potential propagation in complex terminal arborizations. *Biophys. J.* 58:1389-1399.
- Parnas, I., and I. Segev. 1979. A mathematical model for conduction of action potentials along bifurcating axons. *J. Physiol. (Lond.)*. 295:323-343.
- Raymond, S. A., and J. Y. Lettvin. 1978. After effects of activity in peripheral axons as a clue to nervous coding. In *Physiology and Pathobiology of Axons*. S. G. Waxman, editor. Raven Press, New York. 203-225.
- Sabah, N. H., and K. N. Leibovic. 1972. The effect of membrane parameters on the properties of the nerve impulse. *Biophys. J.* 12:1132-1144.
- Scriven, D. R. L. 1981. Modelling repetitive firing and bursting in a small unmyelinated nerve fiber. *Biophys. J.* 35:715-730.
- Skaugen, E. 1980. Firing behaviour in nerve cell models with a two-state pore system. *Acta Physiol. Scand.* 109:377-392.
- Skaugen, E., and L. Walløe. 1979. Firing behaviour in a stochastic nerve membrane model based upon the Hodgkin-Huxley equations. *Acta Physiol. Scand.* 107:343-363.
- Stockbridge, N. 1988. Differential conduction at axonal bifurcations. II. Theoretical basis. *J. Neurophysiol. (Bethesda)*. 59:1286-1295.
- Stockbridge, N., and L. L. Stockbridge. 1988. Differential conduction at axonal bifurcations. I. Effect of electrotonic length. *J. Neurophysiol. (Bethesda)*. 59:1277-1285.
- Swadlow, H. A., J. D. Kocsis, and S. G. Waxman. 1980. Modulation of impulse conduction along the axonal tree. *Annu. Rev. Biophys. Bioeng.* 9:143-179.
- Waxman, S. G., and J. M. Ritchie. 1985. Organization of ion channels in the myelinated nerve fiber. *Science (Wash. DC)*. 228:1502-1507.